ノートのタイトル 2008/03/07

乱流のマルティフラクタルPDF解析とその周辺

有光敏彦（筑波大数理）

協同研究者：

有光直子（横国大環情）
吉田　恭（筑波大数理）
毛利英明（気象研究所）
本池　巧（湘北短大）

ノートのタイトル 2007/12/16

0. 乱流とは

図 1: Leonardo da Vinciによる乱流のスケッチ。
（1513）

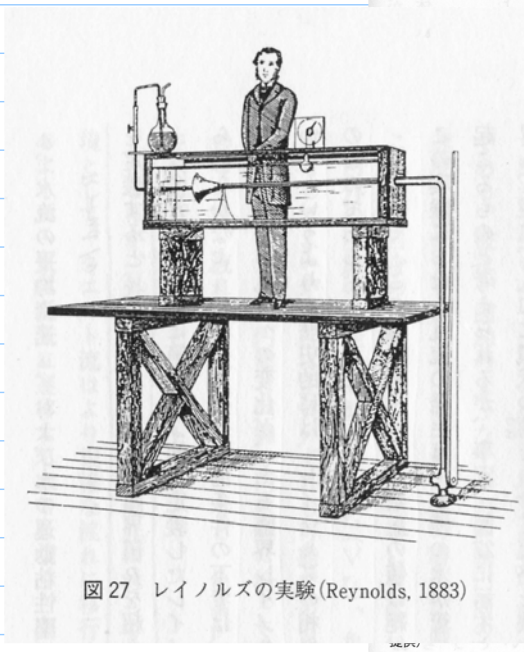

図27　レイノルズの実験（Reynolds, 1883）

「パラドックスとしての流体」巽 友正
（培風館, 1996）より転載。

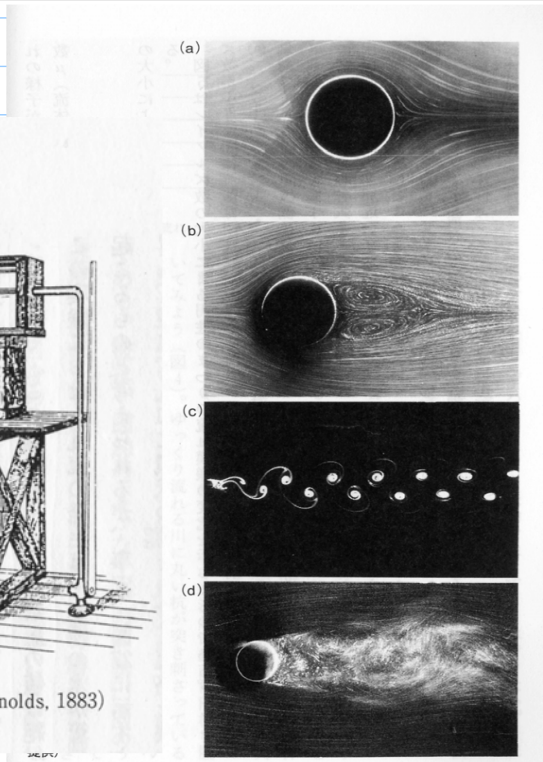

「いまさら流体力学？」木田重雄
（丸善, 1994）より転載。

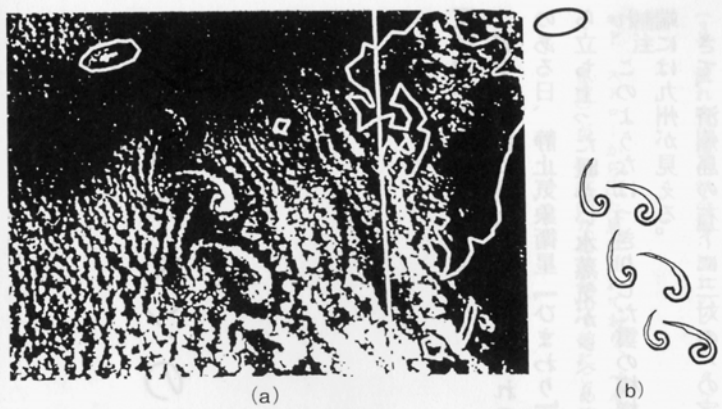

▲図1　済州島付近のカルマン渦列
(a) 静止気象衛星『ひまわり』から見た九州西方海上の雲の分布．1983年12月4日．丸く囲った島(済州島)の右下に3対のハの字型の雲が見える．(b) 反対向きに回転している渦が互い違いに並んでいる．

「いまさら流体力学？」木田重雄
(丸善, 1994) より転載。

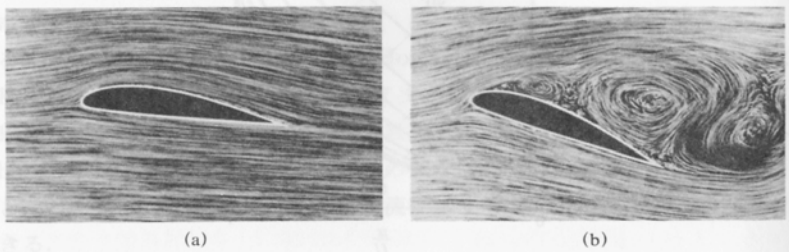

図 15·10　境界層の剝離　(a) 剝離なし，(b) 全面的剝離．

「流体力学」巽 友正（新物理学シリーズ21，培風館, 1982）より転載。

1. 乱流と Kolmogorov 41

乱流の基礎方程式

kinematic viscosity　乱雑力

$$\frac{\partial \underset{\sim}{u}}{\partial t} + (\underset{\sim}{u}\cdot\underset{\sim}{\nabla})\underset{\sim}{u} = -\underset{\sim}{\nabla} p + \nu \nabla^2 \underset{\sim}{u} + \underset{\sim}{f}$$

圧力/密度

Navier-Stokes equation

$$\underset{\sim}{\nabla}\cdot\underset{\sim}{u} = 0$$

非圧縮性

間欠性

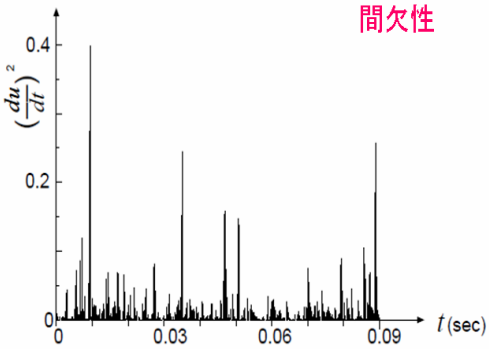

図 6: $\nu u'^2$ に比例する量 $(\partial u/\partial t)^2$ (cm^2/sec^4) の時間変化 (毛利らが風洞実験で得た速度場の時系列データを利用)。

充分発達した乱流を扱い，
間欠性の本質に迫る

A typical setup of the observation of fully developed turbulence behind a grid in a wind tunnel

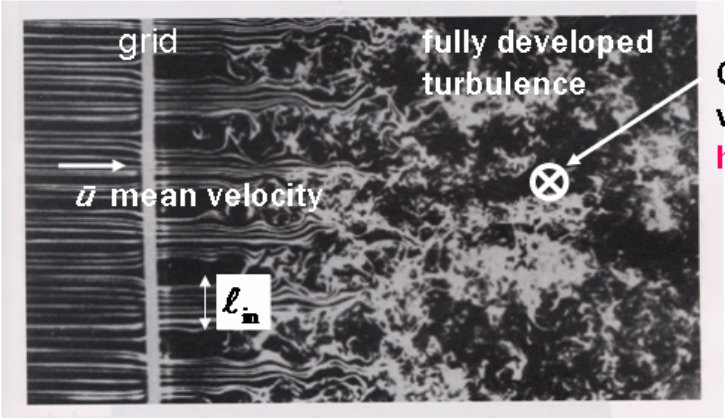

M. Van Dyke, *An Album of Fluid Motion* (The Parabolic Press, Stanford, California, 1982) より転載。

Observe the wind velocities $u(t)$ by a x-array hot wire prove.

by Mouri (2004)
$R_\lambda = 249$,
$\bar{u} = 10$ [m/sec]
$\ell_{in} \approx 20$ [cm]

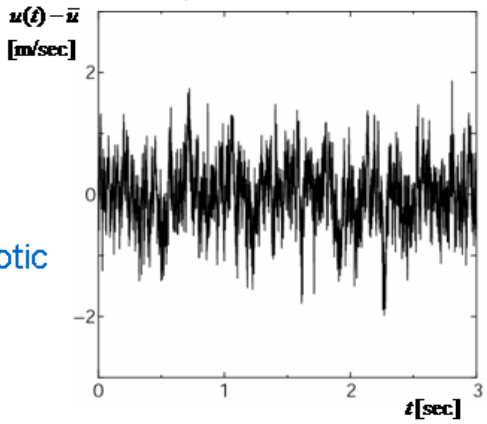

The observed time series of the longitudinal velocity component $u(t)$-$\bar{u}$ represents its chaotic changes in time.

The velocity differences $\delta u(t;\delta t) = u(t+\delta t) - u(t)$ for $\delta t = 3.3\text{x}10^{-5}$ [sec] and $\delta t = 1.3\text{x}10^{-2}$ [sec] are shown. The former represents intermittent character, whereas the latter looks like mere fluctuating behavior.

The velocity differences are scaled by their standard deviations:

$$\xi(t;\delta t) = \delta u(t;\delta t) \Big/ \sqrt{\langle \delta u(t;\delta t)^2 \rangle}$$

With the help of the Taylor frozen hypothesis, we can translate the time difference δt into the spatial distance r by the relation, $r = \bar{u}\,\delta t$.

Kolmogolov scale: $\eta = 0.22$ [mm].

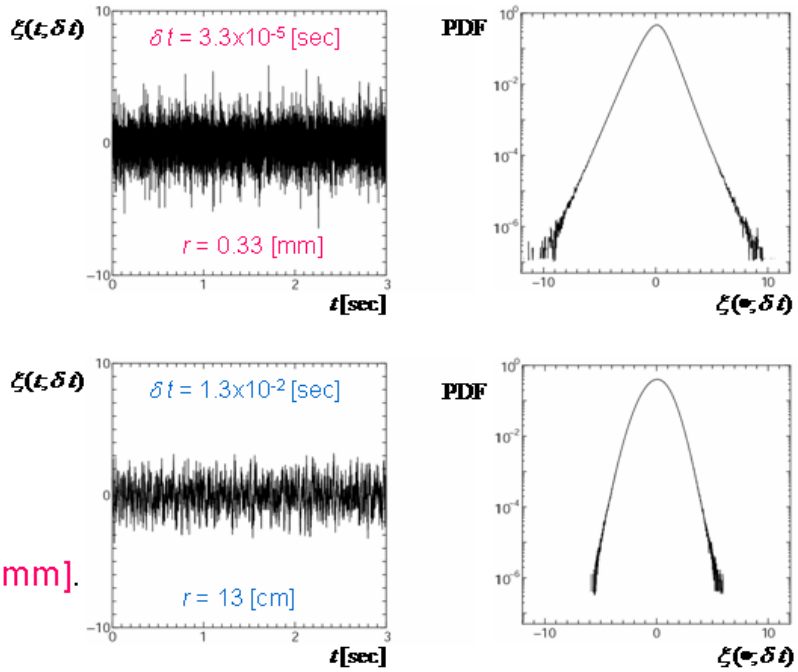

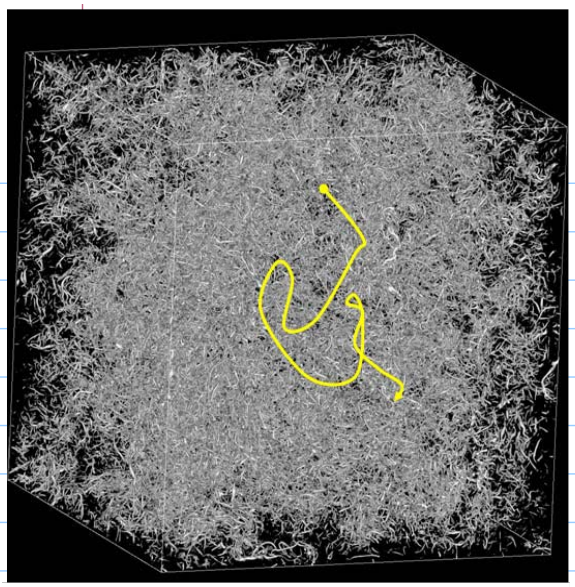

DNS by M. Tanahashi (TIT) at $Re_\lambda = 220.7$

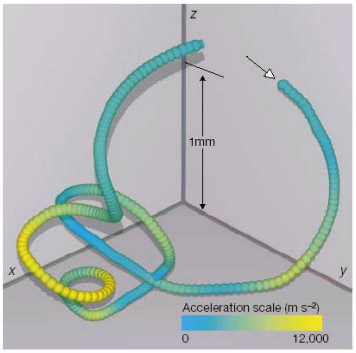

A. La Porta et al., Nature **409** (2001) 1017.

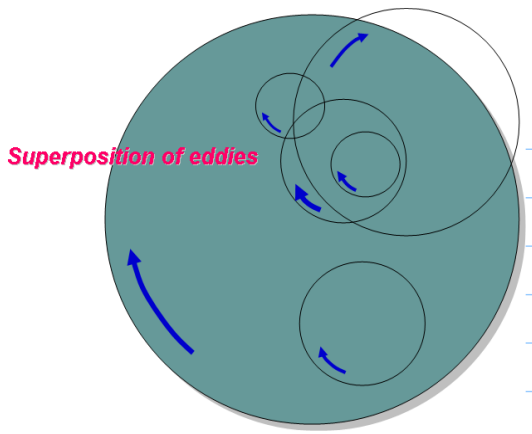

Now, the velocity differences

$$\delta u_n = \left| u(\bullet + \ell_n) - u(\bullet) \right|$$

are measured at every two points separated by ℓ_n.

In the following, we will measure the spatial distance r by the discrete units

$$r = \ell_n = \delta_n \ell_0 \quad (\delta_n = 2^{-n})$$

specified by the number n of the multifractal depth.
(The values of n can be positive real number in the analysis of experiments).

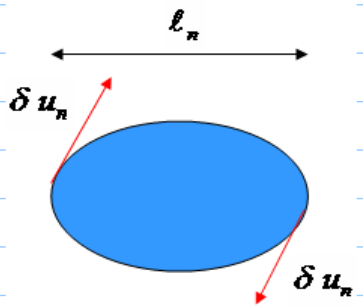

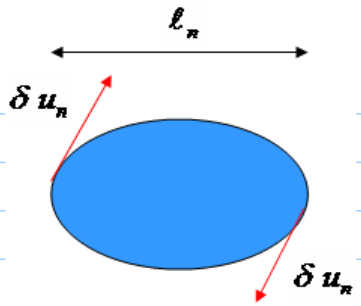

$$t_n = \frac{\ell_n}{|\delta u_n|}$$: characteristic time necessary for an eddy to rotate once

$$t_n^{diss} = \frac{\ell_n^2}{\nu}$$: characteristic time required for energy of an eddy to dissipate into heat

$$E_n = \int_{k_n}^{k_{n+1}} dk\, E(k) = \frac{\delta u_n^2}{2}$$: kinetic energy of eddies per unit mass with diameters in the range $\ell_n \sim \ell_n + d\ell_n$

$$|\delta \epsilon_n| = \frac{E_n}{t_n} = \frac{|\delta u_n|^3}{\ell_n}$$: energy transfer rate from the eddies with diameter ℓ_n to the eddies with ℓ_{n+1}

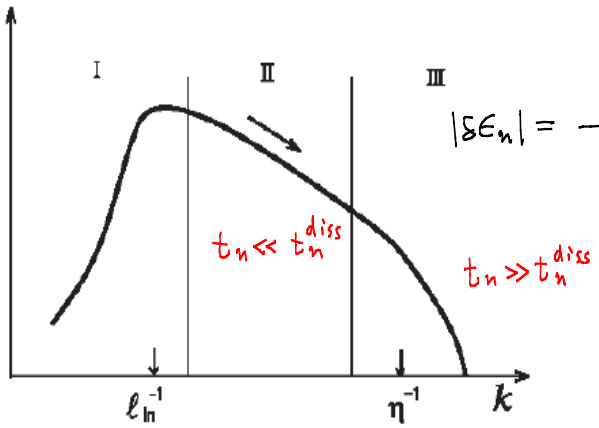

Figure 1. I: the energy input range, II: the inertial range, and III: the dissipation range.

$t_n \ll t_n^{diss}$ では、エネルギー散逸が効かず大きい渦から小さい渦にエネルギーが遷移する。 energy cascade

Kolmogorov (K41)

Energy cascade

エネルギー注入率 ϵ

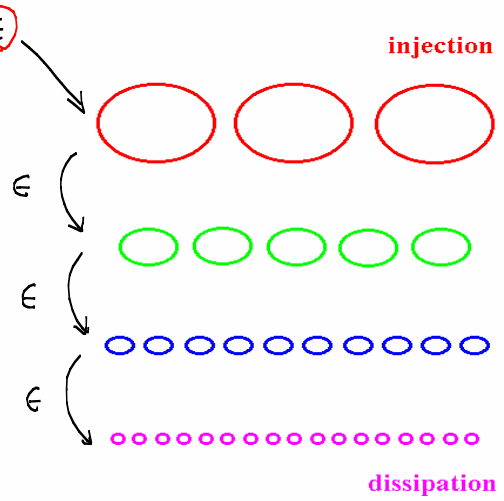

At each step, the eddies are space filling.

$$|\delta \epsilon_n| = \epsilon$$

$$|\delta u_n| = (\epsilon\, l_n)^{1/3}$$

$$t_n = \frac{l_n}{|\delta u_n|} = \frac{l_n^{2/3}}{\epsilon^{1/3}}$$

$$t_n = t_n^{diss} \longrightarrow l_n \equiv \eta$$

$$\eta = \left(\frac{\nu^3}{\epsilon}\right)^{1/4}$$

Kolmogorov length

$$E_n = E(k_n)\, k_n \sim (\delta u_n)^2 = (\epsilon\, l_n)^{2/3}$$

$$\boxed{E(k_n) \sim \epsilon^{2/3}\, k_n^{-5/3}}$$

Kolmogorov spectrum

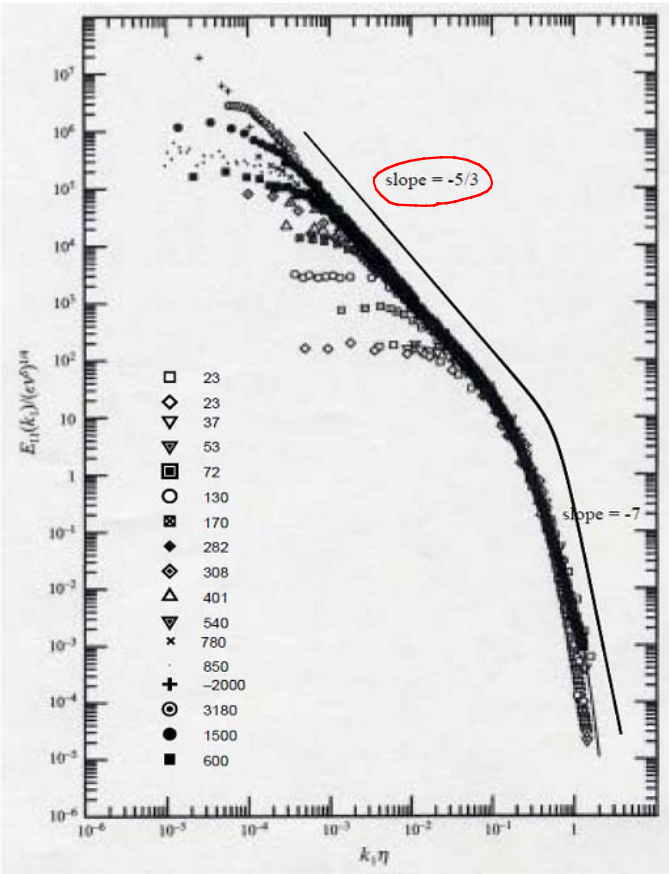

S.G. Saddoughi and S.V. Veeravalli, *J. Fluid Mech.* **268** (1994) 333.

$$\boxed{E(k_n) \sim \epsilon^{2/3}\, k_n^{-5/3}}$$

Kolmogorov spectrum

$$E_k = K_0 \left(\epsilon\nu^5\right)^{1/4} (k\eta)^{-5/3} \left[1 + \frac{27K_0^3}{8}(k\eta)^4\right]^{-4/3}$$

Heisenberg spectrum

2. N-S方程式とスケール不変性

$$\frac{\partial \underset{\sim}{u}}{\partial t} + \underbrace{(\underset{\sim}{u}\cdot\underset{\sim}{\nabla})\underset{\sim}{u}}_{\text{対流項}} = -\underset{\sim}{\nabla} p + \underbrace{\nu \nabla^2 \underset{\sim}{u}}_{\text{散逸項}}$$

Reynolds 数

$$Re = \frac{[\text{対流項}]}{[\text{散逸項}]} = \frac{\dfrac{(\delta u_0)^2}{\ell_0}}{\nu \dfrac{\delta u_0}{\ell_0^2}}$$

$$= \frac{\ell_0 \delta u_0}{\nu}$$

空気の動粘性係数 $\nu = 1.5 \times 10^{-5}\ m^2/sec$
(20°C 1気圧)

人の歩く早さを時速 4 Km/hour とすると, $U = 1.1\ m/sec$

人の肩巾を 60 cm とすると $L = 0.6\ m$

$Re = 4 \times 10^4$ $Re \geq 10^3$ で乱流が発生する

人が普通に歩いていると, 背後に乱流が発生している。

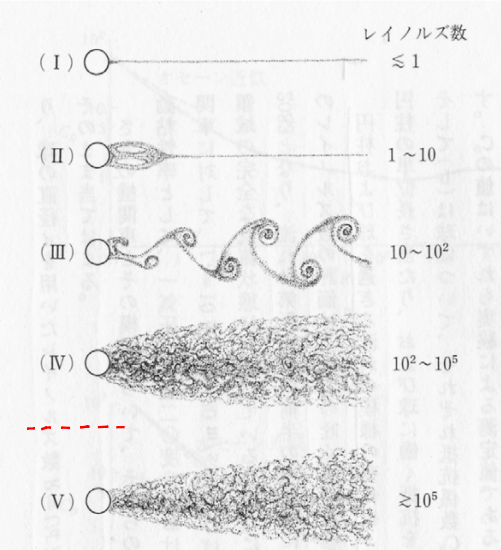

図22 円柱を過ぎる流れのレイノルズ数による変化
「パラドックスとしての流体」巽 友正(培風館, 1996)

$$\frac{\partial \underset{\sim}{u}}{\partial t} + (\underset{\sim}{u}\cdot\underset{\sim}{\nabla})\underset{\sim}{u} = -\underset{\sim}{\nabla} p + \nu \nabla^2 \underset{\sim}{u}$$

For high Raynolds number $\mathrm{Re} = \frac{\delta u_0 \ell_0}{\nu} >> 1$,
it is invariant under the scale transformation (α : real)

α は任意!!

$$\vec{r} \to \lambda \vec{r},\ \vec{u} \to \lambda^{\alpha/3}\vec{u},\ t \to \lambda^{1-\alpha/3} t,\ \frac{p}{\rho} \to \lambda^{2\alpha/3}\frac{p}{\rho}.$$

With the length $\ell_n = \delta_n \ell_0$ $(\delta_n = 2^{-n})$, these quntities are given as follows.

$$|\vec{u}'| = \lim_{n\to\infty} u'_n = \lim_{\ell_n \to 0} \frac{\delta u_n}{\ell_n} \sim \lim_{\ell_n \to 0} \ell_n^{\frac{1}{3}\alpha - 1}, \qquad \delta u_n = |u(\bullet + \ell_n) - u(\bullet)|,$$

$$|\vec{a}| = \lim_{n\to\infty} a_n = \lim_{\ell_n \to 0} \frac{\delta p_n}{\ell_n} \sim \lim_{\ell_n \to 0} \ell_n^{\frac{2}{3}\alpha - 1}, \qquad \delta p_n = |(p/\rho)(\bullet + \ell_n) - (p/\rho)(\bullet)|,$$

$$\varepsilon_\infty = \lim_{n\to\infty} \varepsilon_n = \lim_{\ell_n \to 0}\left(\frac{\ell_n}{\ell_0}\right)^{\alpha-1} \sim \lim_{\ell_n \to 0} \ell_n^{\alpha - 1}$$

where $\vec{a} = \frac{\partial \vec{u}}{\partial t} + (\vec{u}\cdot\vec{\nabla})\vec{u}$ is the acceleration of fluid particle.

The velocity derivative, the acceleration and the energy transfer rate become, respectively, singular for $\alpha < 3$, $\alpha < 1.5$ and $\alpha < 1$ in the limit $\ell_n \to 0$.

When $\alpha < 1$, all these three quantities become large for each ℓ_n.

3. Landau の批判と Kolmogorov 62 (Log-normal model)

エネルギー遷移率 $\delta\epsilon_n$ は，確率変数として扱うべき (Landau 1944)。

⇓

サイズ ℓ_n の領域での散逸率 ε_n を確率変数と考える (K62)。

$$\varepsilon_n \sim \delta\epsilon_n$$

Kolmogorov (K41)

Energy cascade

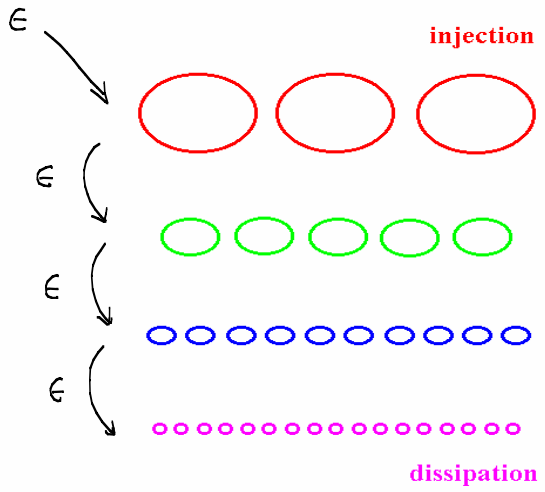

At each step, the eddies are space filling.

4. 異常性指数のマルチフラクタル分布

Eddies with size ℓ_n painted by the same color carry singularity labeled by α, and occupy real space with the fractal dimension $f(\alpha)$.

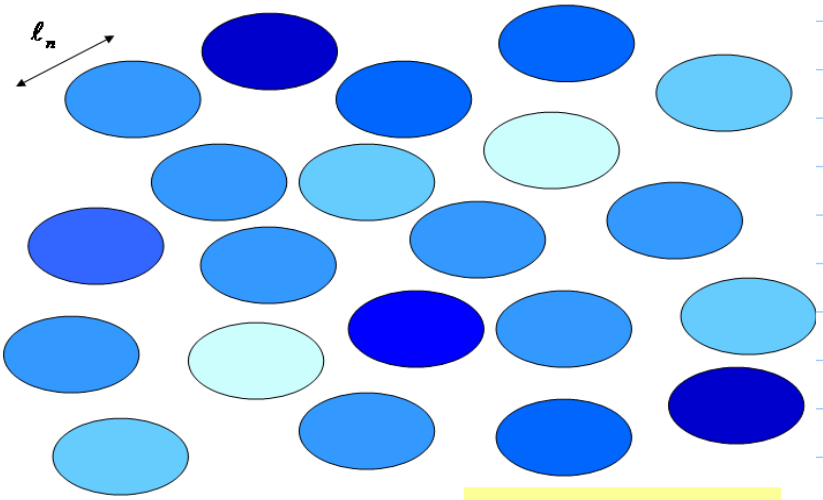

Origin of intermittency

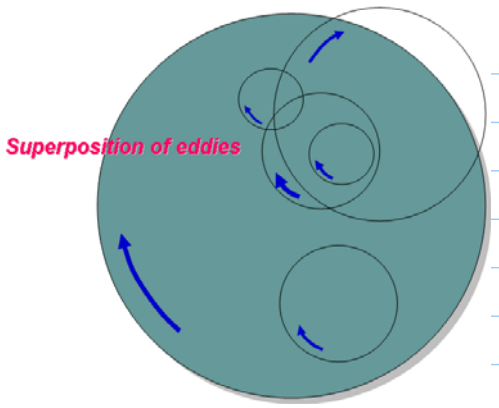

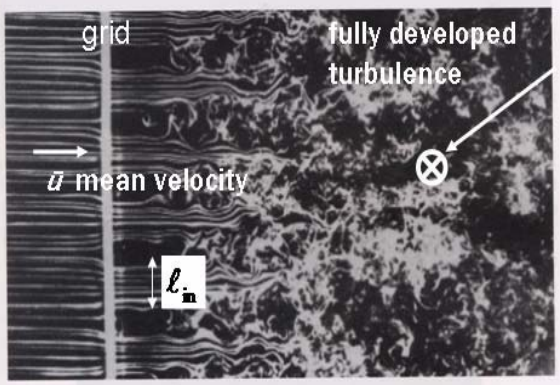

M. Van Dyke, *An Album of Fluid Motion* (The Parabolic Press, Stanford, California, 1982) より転載。

4.1 Basics of multifractal theory

$$\delta u_n = u(\cdot + l_n) - u(\cdot)$$

速度場の1成分

$l_n = l_0 \delta_n$

$\delta_n = \delta^{-n} \quad (\delta > 1)$

$$\epsilon_n = \frac{|\delta u_n|^3}{l_n}$$: energy dissipation rates

Invariance of Navier-Stokes eq. under the scale transformation:

$$\vec{x} \to \vec{x}' = \lambda \vec{x}, \quad \vec{u} \to \vec{u}' = \lambda^{\alpha/3}\vec{u}, \quad t \to t' = \lambda^{1-\alpha/3} t, \quad p \to p' = \lambda^{2\alpha/3} p$$

$$\nu \to \nu' = \lambda^{1+\alpha/3}\nu$$

αは任意の実数

gives us

$$\left|\frac{\delta u_n}{\delta u_0}\right| = \delta_n^{\alpha/3}.$$

Then we have

$$\frac{\epsilon_n}{\epsilon} = \delta_n^{\alpha/3}$$

$\epsilon = \epsilon_0$

Distribution of α :

multifractal spectrum

$$p^{(n)}(\alpha)\, d\alpha = \frac{1}{Z^{(n)}} \delta_n^{d - f_d(\alpha)} d\alpha$$

$$= \frac{[f_d(\alpha)\text{次元空間のうめつくす1辺が}\delta_n\text{の箱の数}]}{[d\text{次元空間をうめつくす1辺が}\delta_n\text{の箱の数}]}$$

$$= \frac{1}{\delta_n^{f(\alpha)}} d\alpha \qquad = \frac{1}{\delta_n^{d}}$$

mass exponents

$$\begin{cases} \tau_d(\bar{q}) = f_d(\alpha) - (\alpha - 1 + d) \\ \bar{q} = \dfrac{d f_d(\alpha)}{d\alpha}, \quad \alpha - 1 + d = -\dfrac{d\tau_d(\bar{q})}{d\bar{q}} \end{cases}$$

Legendre transf.

$$\left\langle \left(\frac{\epsilon_n}{\epsilon}\right)^{\bar{q}} \right\rangle = \left\langle \delta_n^{(\alpha-1)\bar{q}} \right\rangle = \delta_n^{-\tau_d(\bar{q}) + (1-\bar{q})d}$$

$$\tau_d(\bar{q}) = (1-\bar{q}) D_{\bar{q}}$$

generalized dim.

- energy conservation : $\left\langle \dfrac{\epsilon_n}{\epsilon} \right\rangle = 1 \longrightarrow \tau_d(1) = 0$
- def. of the intermittency exponent μ : $\left\langle \left(\dfrac{\epsilon_n}{\epsilon}\right)^2 \right\rangle = \delta_n^{-\mu} \longrightarrow \mu = \tau_d(2) + d$

Scaling exponents ζ_m:

$$\left\langle \left| \frac{\delta u_n}{\delta u_0} \right|^m \right\rangle = \delta_n^{\zeta_m}$$

$$\zeta_m = 1 - \tau_d\left(\frac{m}{3}\right)$$

4.2 Log-normal model

$$\xi_n = \ln \frac{\epsilon_n}{\epsilon_{n-1}} \quad (n = 1, 2, \cdots)$$

(仮) 平均値 $\bar{\xi}$, 分散 σ^2 の共通の確率密度関数

$$\Xi = \frac{1}{\sqrt{n}\,\sigma} \sum_{j=1}^{n} \xi_j, \qquad \bar{\Xi} = \frac{\sqrt{n}}{\sigma} \bar{\xi}$$

$\underline{n \gg 1}$

$$P(\Xi) = \sqrt{\frac{1}{2\pi}}\, e^{-\frac{(\Xi - \bar{\Xi})^2}{2}}$$

中心極限定理

ところで

$$\frac{\epsilon_n}{\epsilon_{n-1}} = \delta^{1-\alpha} \longrightarrow \xi_n = (1-\alpha)\ln\delta$$

$$\bar{\Xi} = \frac{\sqrt{n}}{\sigma}(1-\bar{\alpha})\ln\delta$$

$P^{(n)}(\alpha)\,d\alpha = P(\Xi)\,d\Xi$ より

$$P^{(n)}(\alpha) = \sqrt{\frac{n(\ln\delta)^2}{2\pi\sigma^2}}\, e^{-\frac{n(\alpha-\bar{\alpha})^2}{2\sigma^2/(\ln\delta)^2}}$$

$$f_d(\alpha) = d - \frac{(\alpha-\bar{\alpha})^2}{2\sigma^2/(\ln\delta)^2}$$

$$\tau_d(\bar{q}) = d - (\bar{\alpha} - 1 + d)\bar{q} + \frac{\sigma^2}{2\ln\delta}\bar{q}^2$$

$\tau_d(1) = 0$, $\mu = \tau_d(2) + d$ より

$$\bar{\alpha} = 1 + \frac{\mu}{2}, \quad \sigma^2 = \mu \ln\delta$$

けっきょく

$$f_d(\alpha) = d - \frac{(\alpha - \bar{\alpha})^2}{\mu}$$

$$\tau_d(\bar{q}) = d - \left(\frac{\mu}{2} + d\right)\bar{q} + \frac{\mu}{2}\bar{q}^2$$

$$q = \frac{d f_d(\alpha)}{d\alpha} = -\frac{\alpha - \bar{\alpha}}{\mu}$$

$$\alpha = -\frac{d\tau_d(\bar{q})}{d\bar{q}} = \bar{\alpha} - \mu\bar{q} \longrightarrow \alpha_{\bar{q}=0} = \bar{\alpha} \equiv \alpha_0$$

$$\begin{cases} \alpha_{min} = -\infty \\ \alpha_{max} = +\infty \end{cases} \qquad D_{\bar{q}} = d - \frac{\mu}{2}\bar{q}$$

4.3 Hosokawa's model (Generalized Cantor sets)

$$\tau_d(\bar{q}) = \frac{\ln[p_1^{\bar{q}} + p_2^{\bar{q}}]}{\ln\delta} + (1 - \bar{q})\left(d - \frac{\ln 2}{\ln\delta}\right)$$

$$\delta = 2^{1/(d-\phi)} \qquad p_1 > p_2 > 0$$

$\delta = 2$ のとき
p-model

$$f_d(\alpha) = -\frac{1}{\ln\delta}\left[\frac{\alpha_{max} - \alpha}{2\Delta\alpha}\ln\frac{\alpha_{max} - \alpha}{2\Delta\alpha} + \frac{\alpha - \alpha_{min}}{2\Delta\alpha}\ln\frac{\alpha - \alpha_{min}}{2\Delta\alpha} + \ln 2\right] - d$$

$$f(\alpha_{max}) = f(\alpha_{min}) = \phi, \qquad 2\Delta\alpha = \alpha_{max} - \alpha_{min} = \frac{\ln(p_1/p_2)}{\ln\delta}$$

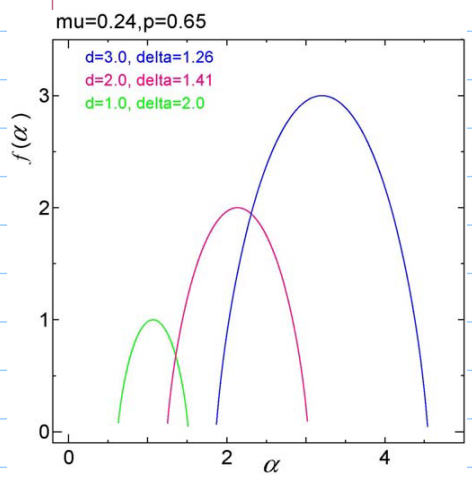

$$\left\langle \frac{\epsilon_n}{\epsilon} \right\rangle = 1 \longrightarrow p_1 + p_2 = 1 \qquad (p_1 \equiv p)$$

$$\left\langle \left(\frac{\epsilon_n}{\epsilon}\right)^2 \right\rangle = \delta_n^{\mu} \longrightarrow p = \frac{1 + \sqrt{\delta^{\mu} - 1}}{2} \qquad \left(p \geq \frac{1}{2}\right)$$

$$p(1-p) = \frac{1}{4}(2 - \delta^{\mu}) > 0$$

$$\downarrow$$

$$\mu < \frac{\ln 2}{\ln\delta}$$

$$\alpha = -\frac{p^{\bar{q}} \ln p + (1-p)^{\bar{q}} \ln(1-p)}{[p^{\bar{q}} + (1-p)^{\bar{q}}] \ln \delta} + d - \frac{\ln 2}{\ln \delta}$$

$$\bar{q} = \frac{\ln(\alpha_{max} - \alpha) - \ln(\alpha - \alpha_{min})}{2\Delta\alpha \ln \delta}$$

$$\begin{cases} \alpha_{min} = -\dfrac{\ln p + \ln 2}{\ln \delta} + d \\ \alpha_{max} = -\dfrac{\ln(1-p) + \ln 2}{\ln \delta} + d \end{cases}$$

$$P^{(n)}(\alpha) = \frac{2^n}{Z^{(n)}} \left[\left(\frac{\alpha_{max} - \alpha}{2\Delta\alpha} \right)^{-\frac{\alpha_{max} - \alpha}{2\Delta\alpha}} \left(\frac{\alpha - \alpha_{min}}{2\Delta\alpha} \right)^{-\frac{\alpha - \alpha_{min}}{2\Delta\alpha}} \right]^n$$

$$\zeta_m = 1 - \tau_d\left(\frac{m}{3}\right)$$

ϕ

dを決めると、μとδの関数!!

δ=2のとき
p-model

4.4 A & A model

$$P^{(n)}(\alpha) = \frac{1}{Z^{(n)}} \left[1 - \frac{(\alpha - \alpha_0)^2}{(\Delta\alpha)^2} \right]^{n/(1-q)}$$

Tsallis type PDF

$$(\Delta\alpha)^2 = \frac{2X}{(1-q)\ln\delta}$$

$$f_d(\alpha) = d + \frac{1}{(1-q)\ln\delta} \ln\left[1 - \frac{(\alpha - \alpha_0)^2}{(\Delta\alpha)^2} \right]$$

$$\bar{q} = \frac{1}{(1-q)\ln\delta} \left(\frac{1}{\alpha - \alpha_{min}} - \frac{1}{\alpha_{max} - \alpha} \right)$$

$$\begin{cases} \alpha_{min} = \alpha_0 - \Delta\alpha \\ \alpha_{max} = \alpha_0 + \Delta\alpha \end{cases}$$

$$\alpha - \alpha_0 = -\frac{2X\bar{q}}{1 + \sqrt{C_{\bar{q}}}}$$

$$C_{\bar{q}} = 1 + 2X\bar{q}^2(1-q)\ln\delta$$

$$\tau_d(\bar{q}) = d - (\alpha_0 - 1 + d)\bar{q} + \frac{2X}{1+\sqrt{C_{\bar{q}}}}\bar{q}^2 + \frac{1}{(1-q)\ln\delta}\left[\ln 2 - \ln\left(1+\sqrt{C_{\bar{q}}}\right)\right]$$

Determination of parmeters α_0, X and q :

$$\left\langle \frac{\epsilon_n}{\epsilon} \right\rangle = 1 \longrightarrow \quad \tau_d(1) = 0 \qquad (1)$$

$$\left\langle \left(\frac{\epsilon_n}{\epsilon}\right)^2 \right\rangle = \delta_n^{-\mu} \longrightarrow \quad \mu = d + \tau_d(2) \qquad (2)$$

Scaling relation:

$$\boxed{\frac{1}{1-q} = \frac{\ln\delta}{\ln 2}\left(\frac{1}{\alpha_-} - \frac{1}{\alpha_+}\right)} \qquad (3)$$

$\frac{\ln\delta}{\ln 2} = \log_2\delta$

本池氏のポスター講演

$$\left(\begin{aligned} & f(\alpha_\pm) = 0 \\ & \alpha_\pm = \alpha_0 \pm \sqrt{2bX} \\ & b = \frac{1}{(1-q)\ln\delta}\left(1 - e^{-d(1-q)\ln\delta}\right) \end{aligned}\right)$$

(3) は

$$\sqrt{2bX} = -(1-q)\log_2\delta + \sqrt{\alpha_0^2 + \left[(1-q)\log_2\delta\right]^2} \qquad (3)'$$

(1) (2) (3′) より

$$\begin{cases} \alpha_0 = \alpha_0(\mu) \\ X = X(\mu) \\ (1-q)\ln\delta = Q(\mu) \end{cases}$$

従って、$\tau_d(\bar{q})$ の係数は、d が決まると、μ だけの関数!!

$\Downarrow$

$\zeta_m = 1 - \tau_d\left(\frac{m}{3}\right)$ も、d が決まると、μ だけの関数!!

μ が与えられたとき、δ を変更しても、$(1-q)\ln\delta = Q(\mu)$ より、q の値が変化するだけで、ζ_m の形は不変!!

entropy index

$$\begin{cases} S^R[P(\alpha)] = \frac{1}{1-q}\ln\int d\alpha\, P(\alpha)^q & : \text{Rény entropy} \\ S^T[P(\alpha)] = \frac{1}{1-q}\left[\int d\alpha\, P(\alpha)^q - 1\right] & : \text{Tsallis entropy} \end{cases}$$

Rényi statistics

q: entropy index

$$S_q = \frac{1}{1-q}\ln\left(\sum_i p_i^q\right)$$

Rényi entropy

$$\sum_i p_i = 1,\ U_q = \frac{\sum_i p_i^q E_i}{\sum_i p_i^q}$$

Stationary state distribution function

$$p_i = \frac{1}{\bar{Z}_q}\left[1-(1-q)\beta(E_i-U_q)\right]^{1/(1-q)} \qquad \bar{Z}_q = \sum_i \left[1-(1-q)\beta(E_i-U_q)\right]^{1/(1-q)}$$

q → 1 gives us the Gibbs.

$$S_q(A+B) = S_q(A) + S_q(B)$$

Havrda-Charvat-Tsallis statistics

q: entropy index

$$S_q = \frac{\sum_i p_i^q - 1}{1-q}$$

HCT entropy

$$\sum_i p_i = 1,\ U_q = \frac{\sum_i p_i^q E_i}{\sum_i p_i^q}$$

Stationary state distribution function

$$p_i = \frac{1}{\bar{Z}_q}\left[1-\frac{(1-q)\beta(E_i-U_q)}{\bar{Z}_q^{1-q}}\right]^{1/(1-q)} \qquad \bar{Z}_q = \sum_i \left[1-\frac{(1-q)\beta(E_i-U_q)}{\bar{Z}_q^{1-q}}\right]^{1/(1-q)}$$

q → 1 gives us the Gibbs.

$$S_q(A+B) = S_q(A) + S_q(B) + (1-q)S_q(A)S_q(B)$$

Multifractal spectrum

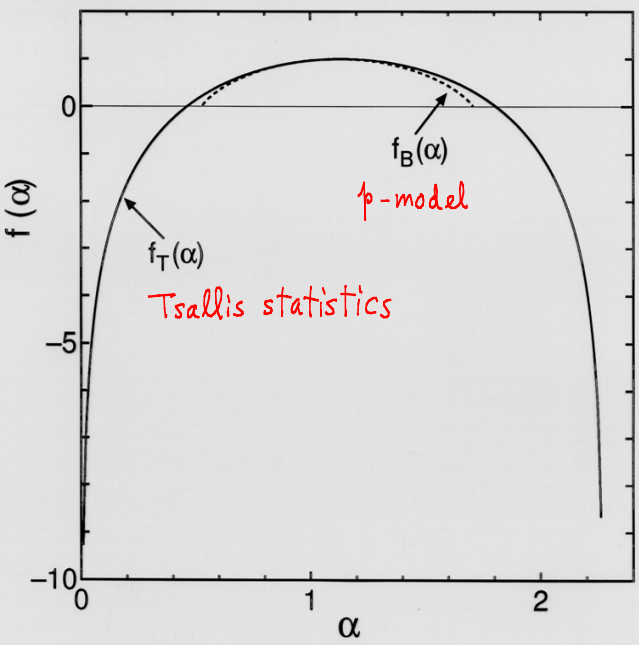

Figure 4: Multifractal spectrum $f_T(\alpha)$ based on Tsallis statistics, and $f_B(\alpha)$ on binomial multiplicative process (p-model), for the case $\mu = 0.235$.

$d=1,\ \delta=2$

δを変更しても、ζ_mの形が変化しないのは、A&A modelだけ!!

Scaling exponents ζ_m of velocity structure function

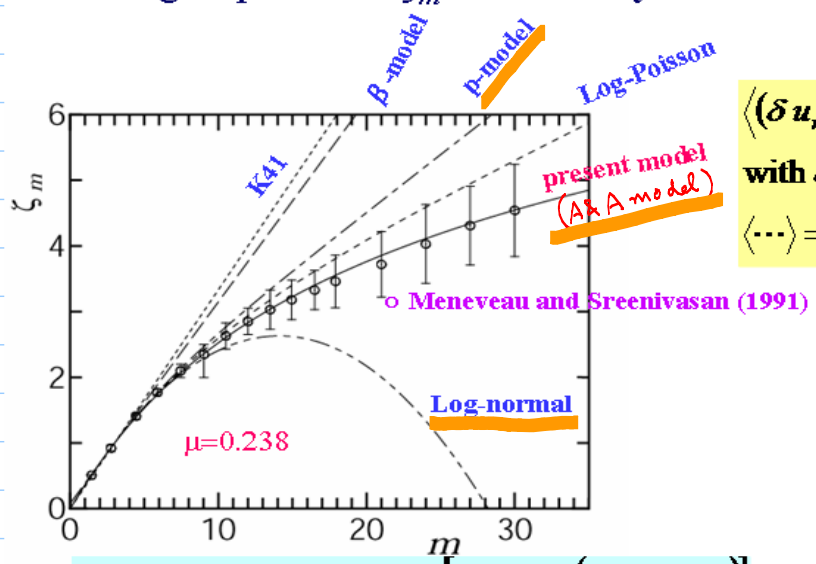

$$\langle (\delta u_n)^m \rangle \propto \ell_n^{\zeta_m}$$

with $\delta u_n = |u(\bullet + \ell_n) - u(\bullet)|$,

$$\langle \cdots \rangle = \int d\alpha \cdots P(\alpha).$$

$$\zeta_m = \frac{\alpha_0 m}{3} - \frac{2X m^2}{9(1+\sqrt{C_{m/3}})} - \frac{1}{1-q}\left[1 - \log_2\left(1+\sqrt{C_{m/3}}\right)\right]$$

with

$$C_{\bar{q}} = 1 + 2X\,\bar{q}^2(1-q)\ln 2$$

$$\sqrt{2X} = \frac{\sqrt{\alpha_0^2 + (1-q)^2} - (1-q)}{\sqrt{b}},\quad b = \frac{1-2^{q-1}}{(1-q)\ln 2}.$$

present model (2000)
(A&A model)

K41 (1941)

$\zeta_m = m/3$

Log-normal (1962)

$\zeta_m = m/3 - \mu m(m-3)/18$

β-model (1978)

$\zeta_m = m/3 - \mu(m-3)/3$

p-model (1987)

$\zeta_m = 1 - \log_2[p^{m/3} + (1-p)^{m/3}]$

$p = (1 + (2^{\mu} - 1)^{1/2})/2$

Log-Poisson (1994)

$\zeta_m = m/9 + 2(1 - (2/3)^{m/3})$

5. マルチフラクタルPDF解析

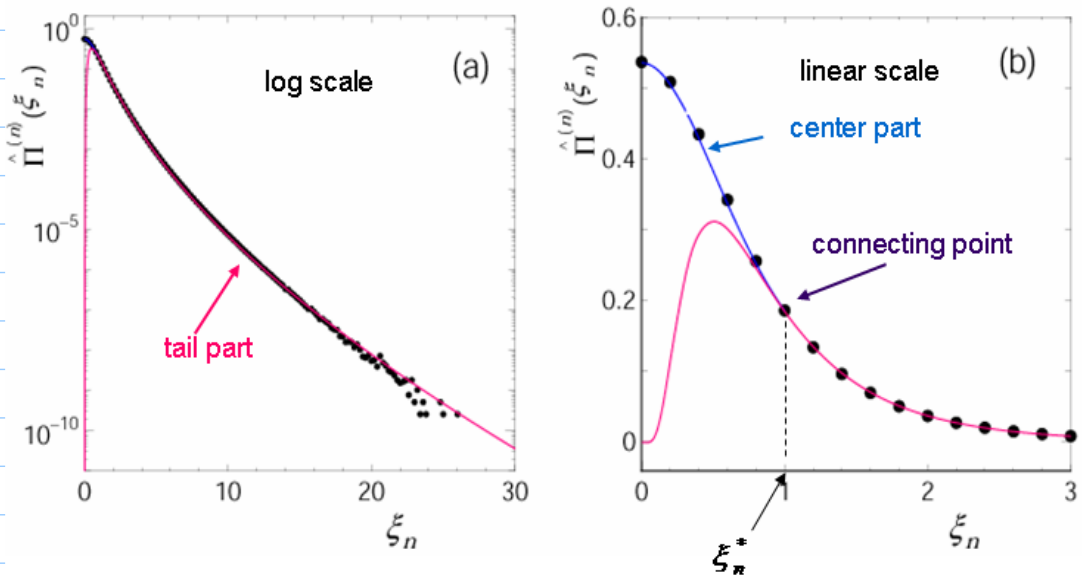

It is revealed in the analyses of experimental data that there are two mechanisms contributing to the PDFs, i.e,

- one is for the **tail part**, and
- the other for the **center part**.

$\hat{\Pi}^{(n)}(\xi_n)\,d\xi_n \propto P^{(n)}(\alpha)\,d\alpha$

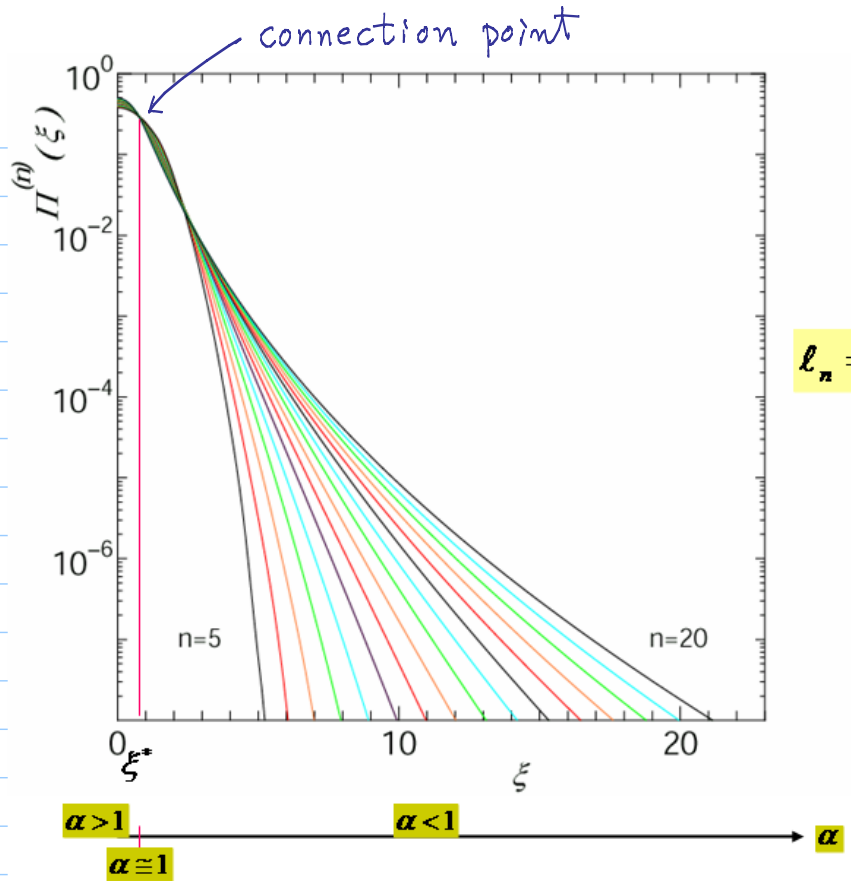

$\ell_n = \delta_n \ell_0 \quad (\delta_n = 2^{-n})$

- Within MFA, the PDF consists of two parts, i.e., the tail part and the center part, divided approximately by the standard deviation.
- The tail part is a manifestation of the multifractal distribution of singularities in physical space due to the scale invariance of the Navier-Stokes equation for large Reynolds number,
  - determined mostly by the intermittency exponent, and
  - representing the intermittent large deviations.
- The center part represents small deviations violating the scale invariance due to the dissipative term in the Navier-Stokes equation proportional to the kinematic viscosity,
  - representing mainly thermal or local fluctuations.

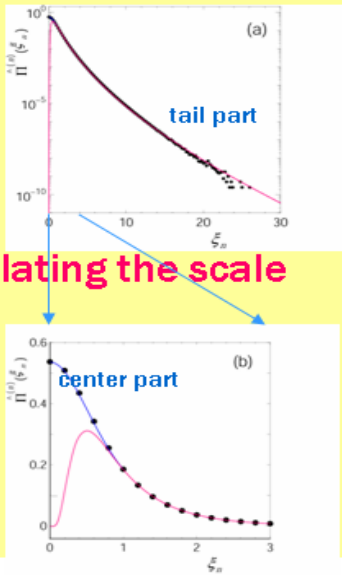

PDF Competition

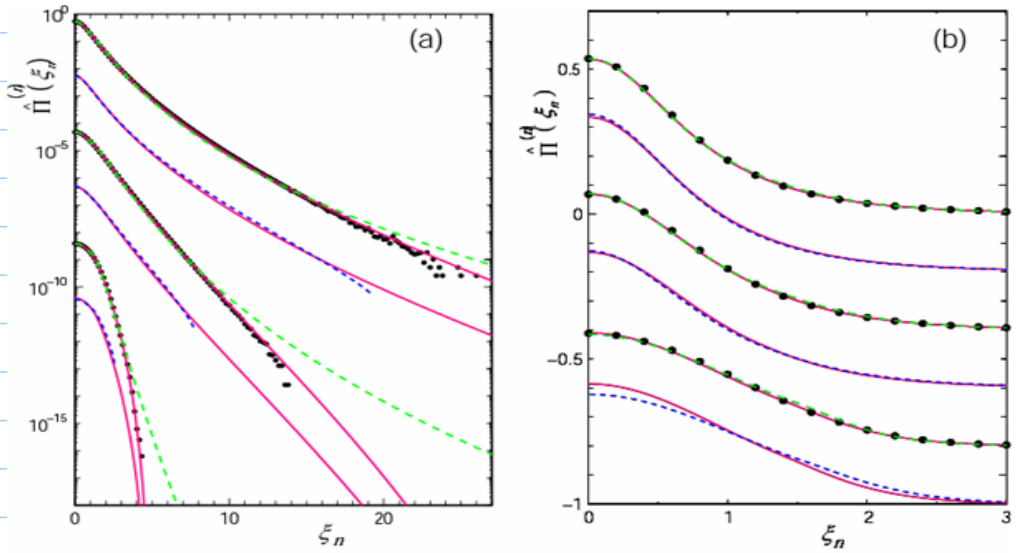

• • • DNS data
— A&A
- - - Log-normal
- - - P model

Fig. 6.5. Analyses of the PDF's of the velocity fluctuations (closed circles) for three different measuring distances, observed by Gotoh et al. at $R_\lambda = 380$, with the help of the PDF's $\hat{\Pi}^{(n)}(\xi_n)$ by the harmonious representation (solid line) and by the log-normal model (dashed line) are plotted on (a) log and (b) linear scales. The PDF's by the p model (dotted line) are compared with the PDF's by the harmonious representation (solid line). Comparisons are displayed in pairs. The solid lines in each set of pairs are the same. For better visibility, each PDF is shifted by -2 unit in (a) and by -0.2 in (b) along the vertical axis. Parameters are given in the text.

$R_\lambda \sim \sqrt{Re}$

6. 実際のデータ解析例

Analysis of experiment conducted by Lewis and Swinney

PDF of velocity fluctuations

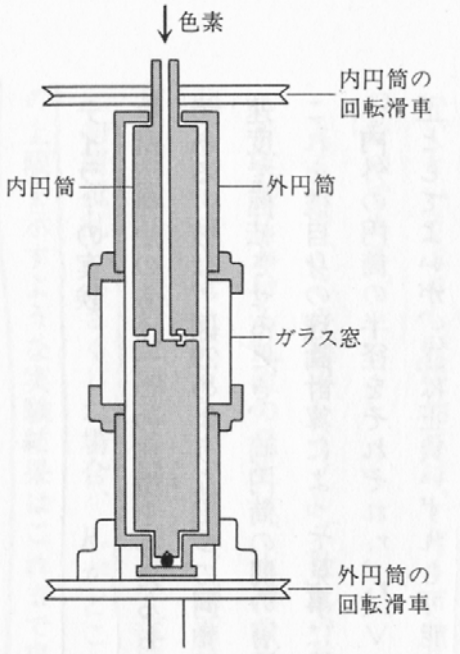

図 29　テイラーの実験(Taylor, 1923)

「パラドックスとしての流体」巽 友正
(培風館, 1996) より転載。

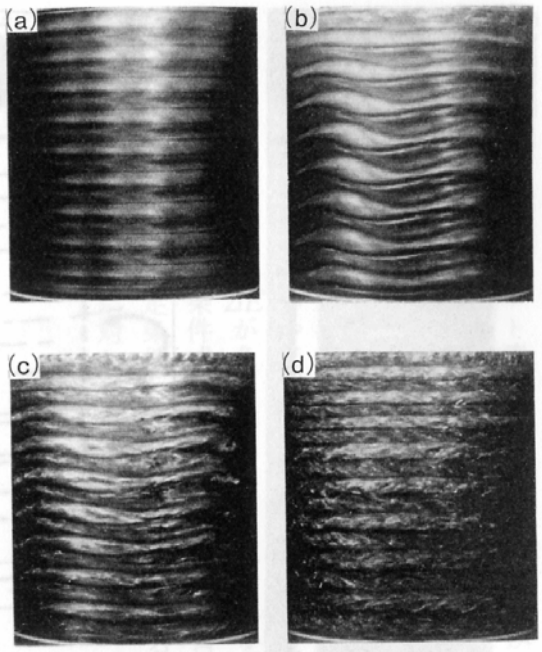

▶図 14　流れのパターンの変化
2 重円筒間の流れで，内側の円筒の回転角速度を徐々に大きくしていくと，まず，(a)定常な軸対称テイラー渦が発生し，それが(b)方位角方向に波打ち始める．さらに進むと，(c)波状テイラー渦に小さな乱れた構造がまつわりつき，(d)乱れの強さが大きくなるとともに縞模様の波は消えていく[7]．

「いまさら流体力学？」木田重雄（丸善, 1994）より転載。

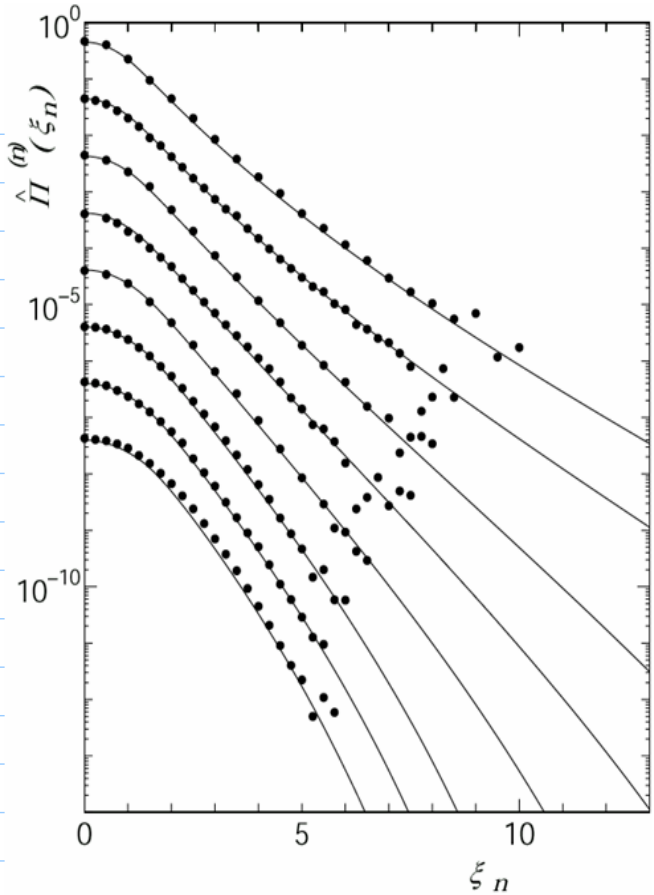

Closed circles
Experimental PDF by Lewis and Swinney (1999)
r/η from top to bottom:
11.6, 23.1, 46.2, 92.5, 208, 399, 830, 1440

Lines
Theoretical PDF with $q = 0.471$ ($\mu = 0.28$) by AA (2001)
n from top to bottom:
14, 13, 11, 10, 9.0, 8.0, 7.5, 7.0

For better visibility, each PDF is shifted by –1 unit along the vertical axis.

Analysis of experiment conducted by Bodenschatz el al.

PDF of fluid particle accelerations

Turbulence chamber (Bodenschatz)

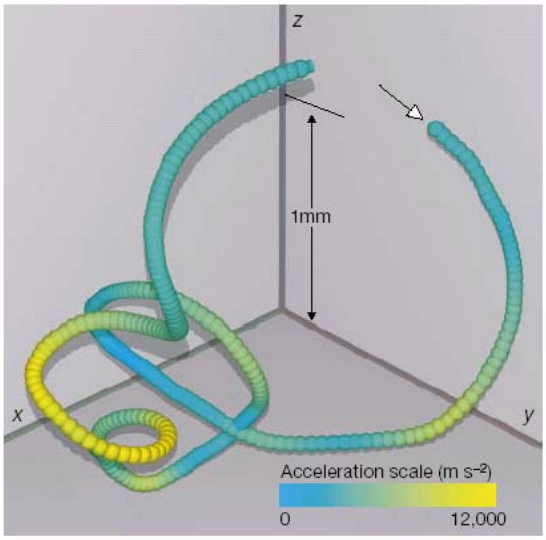

A. La Porta et al., Nature **409** (2001) 1017.

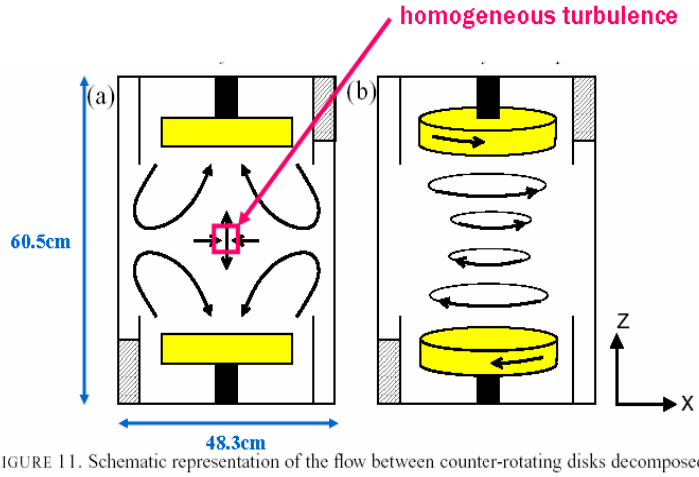

FIGURE 11. Schematic representation of the flow between counter-rotating disks decomposed into (a) the pumping mode and (b) the shearing mode.

G.A. Voth et al., J. Fluid Mech. **469** (2001) 121.

Let us analyze the PDF of particle accelerations observed by Bodenschatz at R_λ=690.

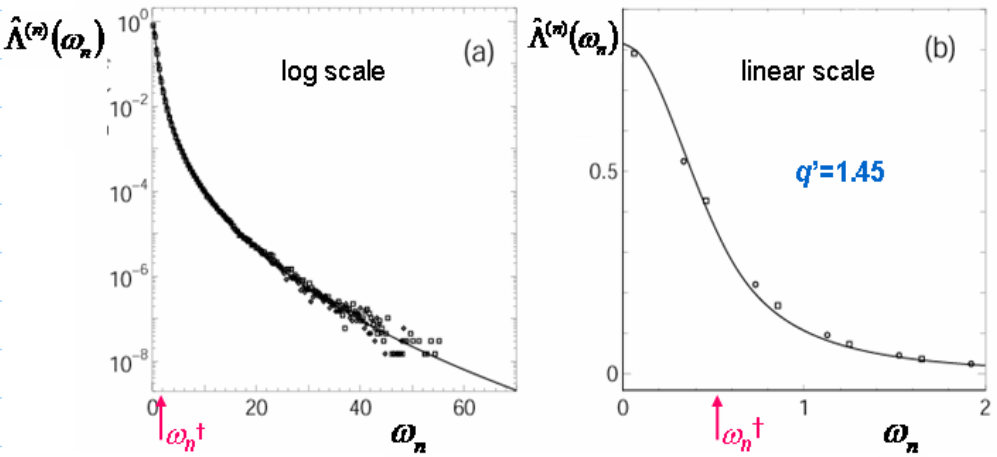

ω_n : acceleration normalized by its deviation

Open squares and circles

Experimental PDF by Bodenschatz et.al (2002)

Lines

Theoretical PDF with q= 0.391 (μ= 0.240) by AA (2002)

$\omega_n^\dagger$= 0.550 $\alpha^\dagger$= 1.01 **n = 17.1**

Analysis of DNS 1024^3 conducted by Gotoh et al

PDF of fluid particle accelerations

PDF of fluid particle accelerations (Gotoh)

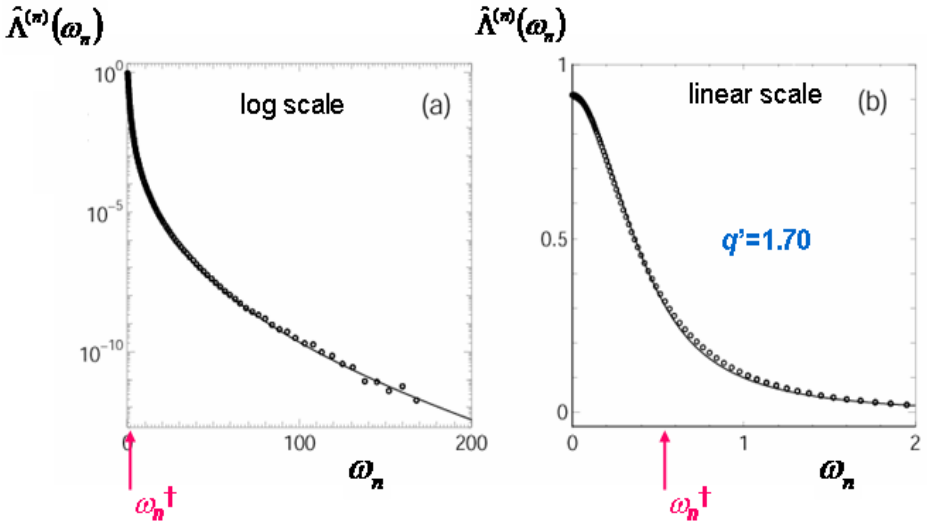

ω_n : acceleration normalized by its deviation

<u>Open squares and circles</u>
Experimental PDF by Gotoh et al. (2002)

<u>Lines</u>
Theoretical PDF with q = 0.391 (μ =0.240) by AA (2002)

$\omega_n^\dagger$ = 0.550 $\alpha^\dagger$= 1.01 n = 17.5

Analysis of DNS 1024^3 conducted by Gotoh et al

PDF of velocity fluctuations

PDF of velocity differences (Gotoh)

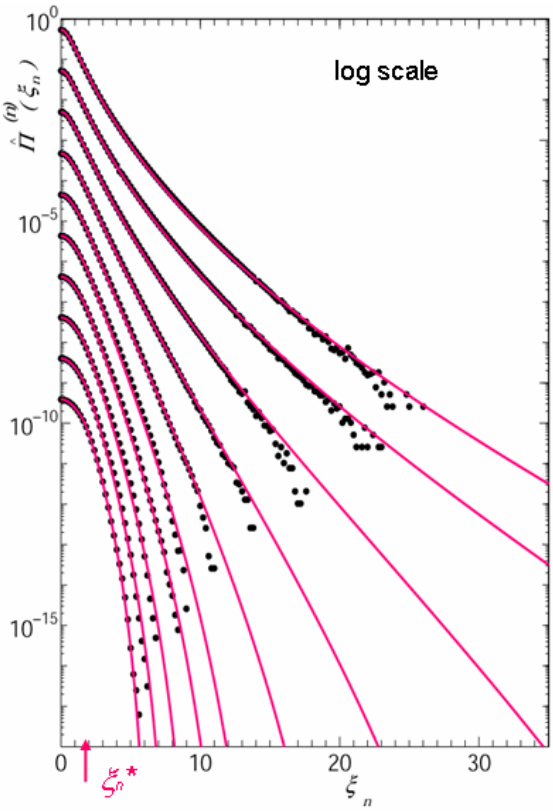

Closed circles
Experimental PDF by Gotoh et al. (2002)
r/η from top to bottom:
2.38, 4.76, 9.52, 19.0, 38.1, 76.2, 152, 305, 609, 1220

Lines
Theoretical PDF with q = 0.391
(μ =0.240) by AA (2001)
n from top to bottom:
20.7, 19.2, 16.2, 13.6, 11.5, 9.80, 9.00, 7.90, 7.00, 6.00
ξ_n^* from top to bottom:
1.10, 1.13, 1.19, 1.23, 1.28, 1.32, 1.34, 1.37, 1.39, 1.43
q' from top to bottom:
1.60, 1.60, 1.58, 1.49, 1.45, 1.40, 1.35, 1.30, 1.25, 1.20
α^*= 1.07
n: number of multifractal steps

For better visibility, each PDF is shifted by −1 unit along the vertical axis.

ξ_n : velocity fluctuation normalized by its deviation

PDF of velocity differences (Gotoh)
Central Part

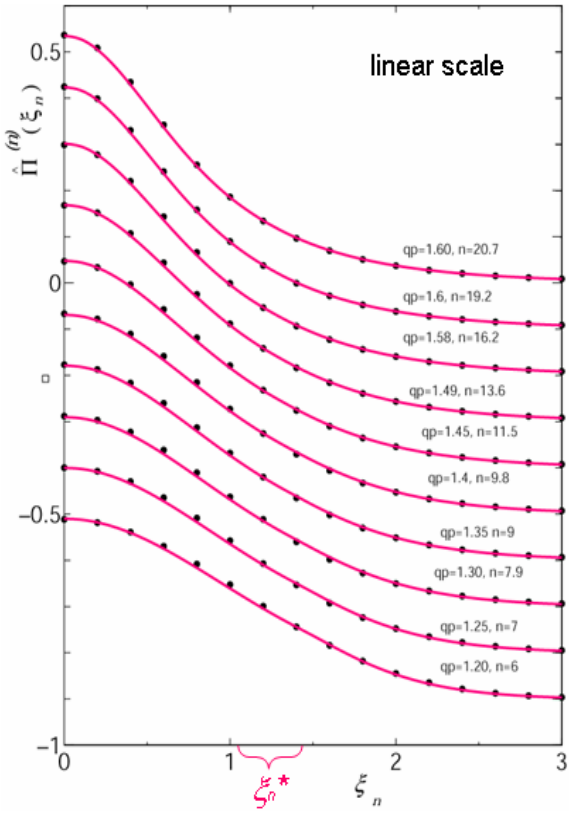

Closed circles
Experimental PDF by Gotoh et al. (2002)
r/η from top to bottom:
2.38, 4.76, 9.52, 19.0, 38.1, 76.2, 152, 305, 609, 1220

Lines
Theoretical PDF with q = 0.391
(μ =0.240) by AA (2001)
n from top to bottom:
20.7, 19.2, 16.2, 13.6, 11.5, 9.80, 9.00, 7.90, 7.00, 6.00
ξ_n^* from top to bottom:
1.10, 1.13, 1.19, 1.23, 1.28, 1.32, 1.34, 1.37, 1.39, 1.43
q' from top to bottom:
1.60, 1.60, 1.58, 1.49, 1.45, 1.40, 1.35, 1.30, 1.25, 1.20
α^*= 1.07
n: number of multifractal steps

For better visibility, each PDF is shifted by −1 unit along the vertical axis.

Analysis of Turbulence in Wind Tunnel measured by Mouri

PDF of energy dissipation rates

$Re = 1.582 \times 10^5$

$R_\lambda = 1258$

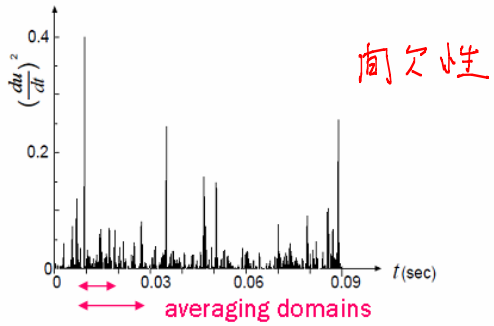

Figure 4: The time dependence of the quantity proportional to $\nu u'^2$ (cm^2/sec^4).

PDF of energy dissipation rates

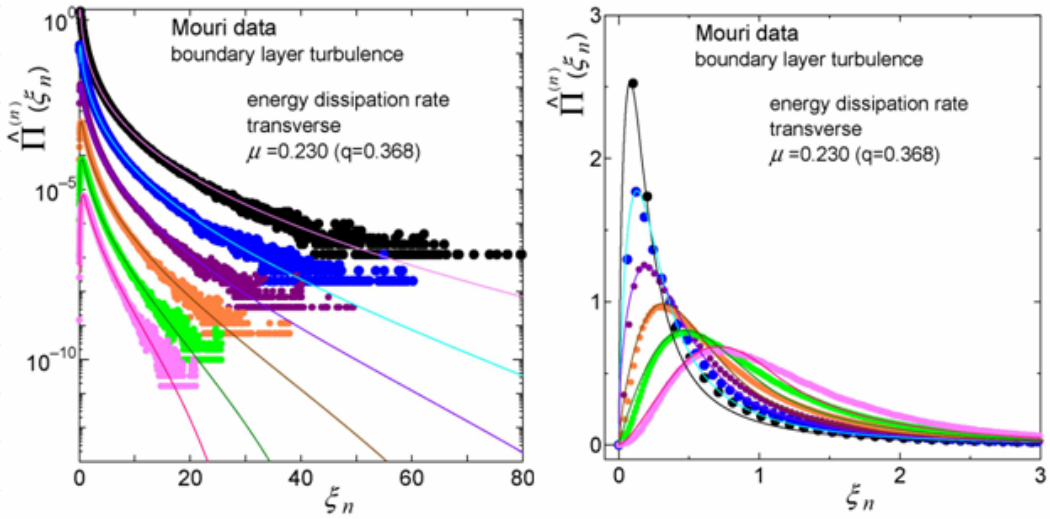

Analysis of DNS 4096^3 conducted by Kaneda et al

PDF of energy dissipation rates

PDF of energy transfer rates

PDFs of energy dissipation rates

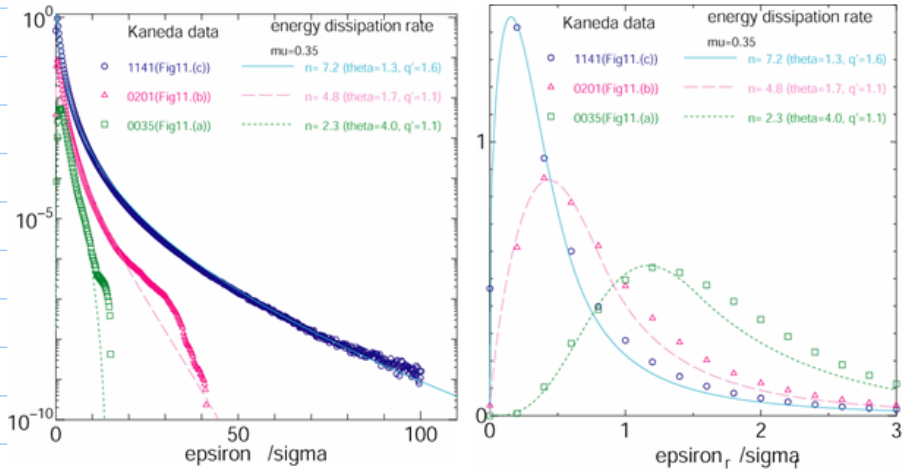

$$n = -0.995 \log_2 r/\eta + 11.1,$$

Closed circles
Experimental PDFs by Kaneda
r/η from top to bottom:
13.7, 78.1, 449
with $\eta = 5.12 \times 10^{-4}$
Inertial range: $62.8 < r/\eta < 224$

Lines
Theoretical PDF with $q = 0.568$
($\mu = 0.345$) by A&A model
(n, q', θ) from top to bottom:
(7.35, 1.59, 1.30), (4.90, 1.10, 1.70), (2.35, 1.10, 4.10)

Connection pts. ξ_n^* from top to bottom:
0.597, 0.839, 1.53 ($\alpha^* = 0.922$)
ξ_n^{max} from top to bottom:
676, 95.7, 14.5

For better visibility, the left PDF is shifted by −1 unit along the vertical axis.

PDFs of energy transfer rates (symmetrized)

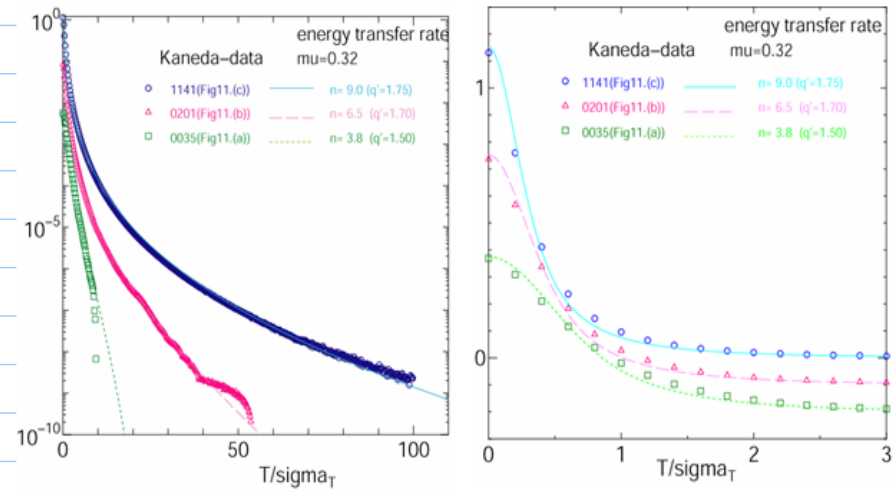

$$n = -1.04 \log_2 r/\eta + 13.0,$$

Closed circles
Experimental PDFs by Kaneda
r/η from top to bottom:
13.7, 78.1, 449
with $\eta = 5.12 \times 10^{-4}$
Inertial range: $62.8 < r/\eta < 224$

Lines
Theoretical PDF with $q = 0.534$
($\mu = 0.320$) by A&A model
(n, q') from top to bottom:
(9.00, 1.75), (6.50, 1.70), (3.80, 1.50)

Connection pts. ξ_n^* from top to bottom:
0.477, 0.637, 0.882 ($\alpha^* = 0.928$)
ξ_n^{max} from top to bottom:
1400, 203, 25.7

For better visibility, the left and right PDFs are respectively shifted by −1 and by - 0.1 unit along the vertical axis.

Analysis of experiment measured in superfluid by Maurer and Tabeling

PDF of velocity fluctuations

Superfluid Turbulence

J.Maurer and P.Tabeling

Europhys. Lett. 43 (1998) 29-34

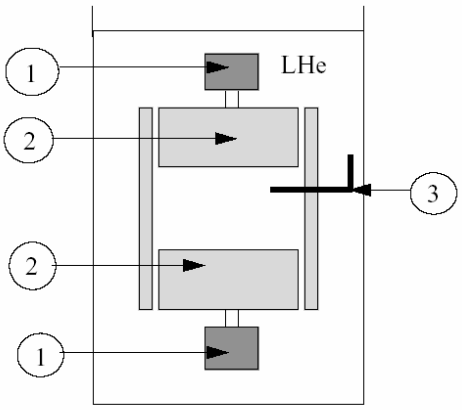

Fig. 1

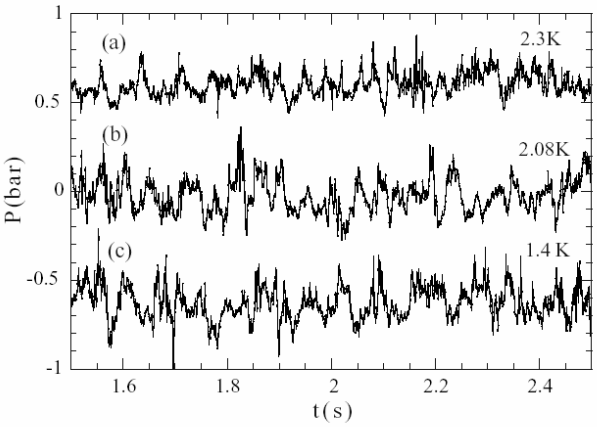

Fig. 2

Fig. 1. – Sketch of the experiment; 1: DC Motor, 2: propellor, 3: probe.

Fig. 2. – Time series obtained for a frequency rotation of 6 Hz, at three different temperatures: (a) 2.3 K (at a 1 bar pressure); (b) 2.08 K; (c) 1.4 K. The time series have been shifted vertically so as to make their representation clear.

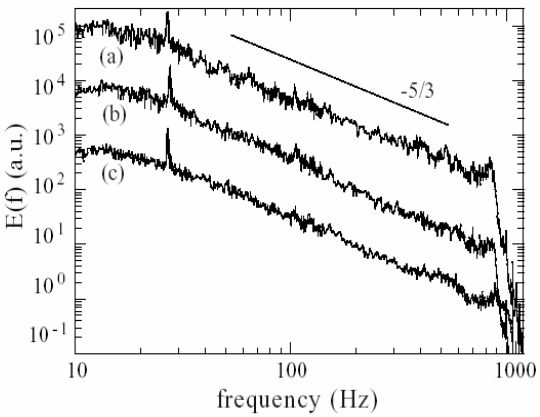

Fig. 3

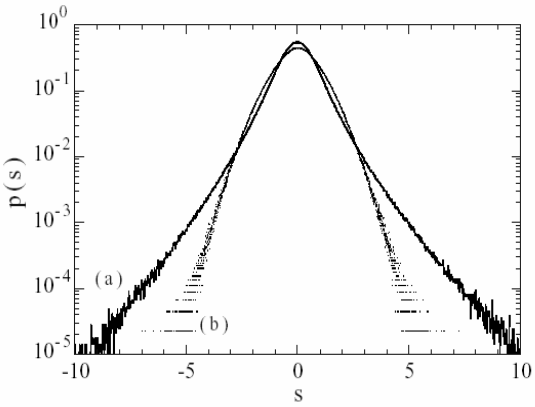

Fig. 4

Fig. 3. – Energy spectra obtained in the same conditions, but at different temperatures: (a) 2.3 K; (b) 2.08 K; (c) 1.4 K. The spectra have been shifted vertically so as to make their representation clear.

Fig. 4. – pdf of the velocity increments obtained for time separations equal to (a) $\delta t = 1$ ms (corresponding to the smallest scale we can resolve) and (b) $\delta t = 100$ ms (which is representative of a large scale), at $T = 1.4$ K; the abcissa s is rescaled so as the variances of the distributions are equal to one.

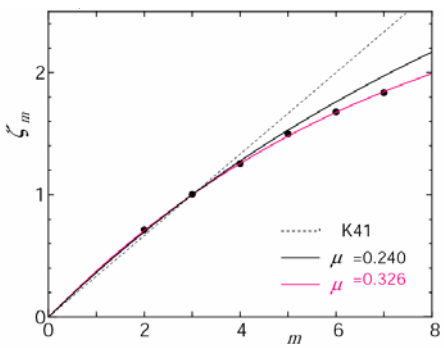

PDF of velocity fluctuations

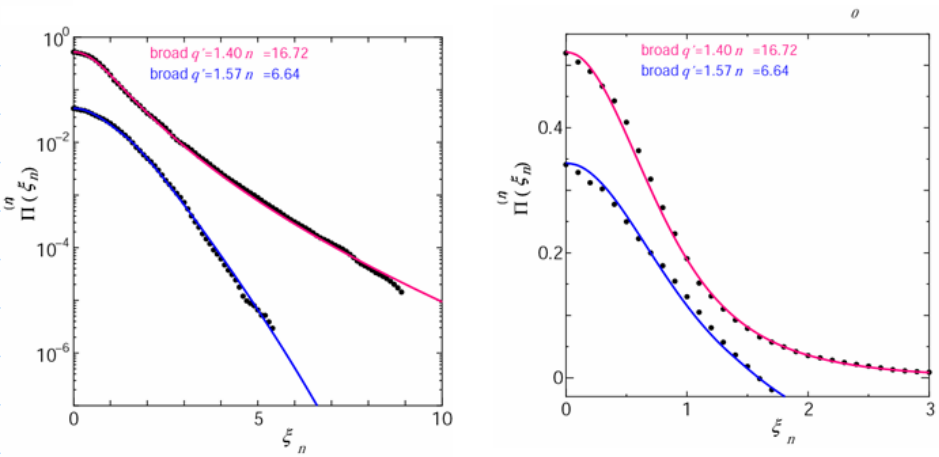

μ =0.326, α_0=0.388, X =1.18 (q =0.543)

Re ~ 2 x 10^6

Analysis of Granurence

PDF of velocity fluctuations

Granular Flow (Granulence)

F. Radjiai and S. Roux, Phys. Rev. Lett. **89** (2002) 064302.

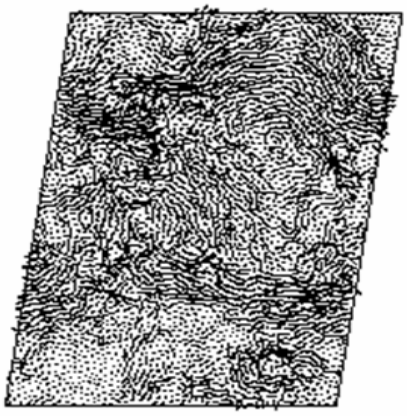

FIG. 1: A snapshot of particle displacements δs^i with respect to the mean background flow.

Minimum time step = 10^{-7}

$$\mathbf{v}^i(t,t+\tau) = \frac{1}{\tau}\int_t^{t+\tau} dt'\, \delta\, \mathbf{s}^i(t')$$

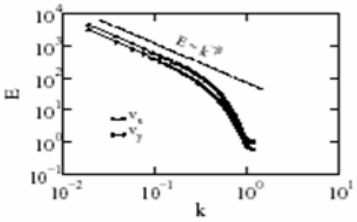

FIG. 4: Averaged power spectrum of the x and y components of the fluctuating velocity field over one time step for one-dimensional cross sections along the mean flow.

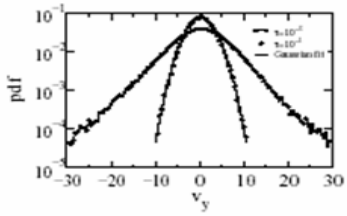

FIG. 2: The pdf's of the y-components of fluctuating velocities for two different integration times: 10^{-3} (broad curve) and 10^{-1} (narrow curve). The latter is fitted by a Gaussian. The error bars are too small to be shown.

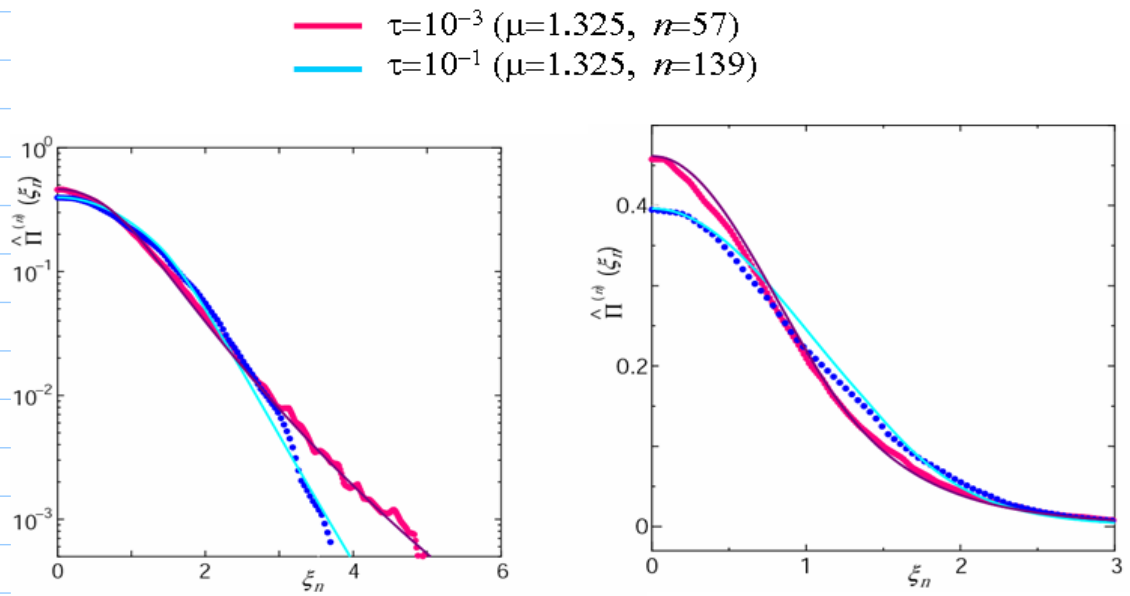

Preliminary analysis in Econophysics

PDF of price changes

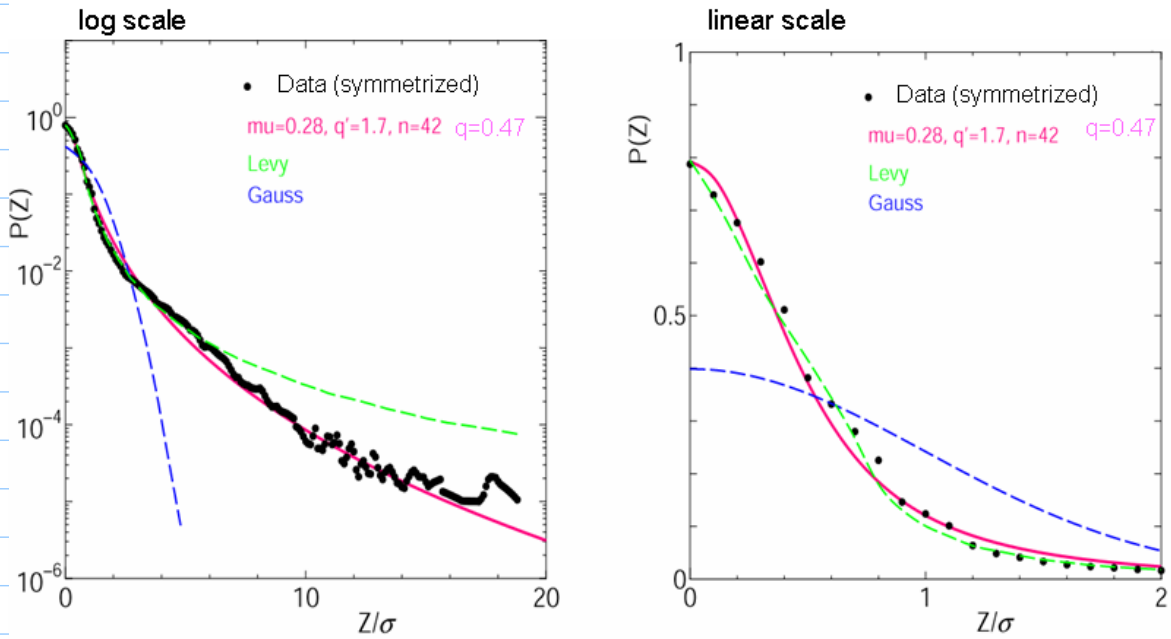

PDF for high-frequency S&P 500 price changes (Mantegna and Stanley, 1995).

8. まとめと今後の問題

It has been revealed that there exist two main contributions to PDFs of those variables representing intermittent large deviations.

The tail part of the PDFs is determined mainly by the global structure of turbulence representing its intermittent character, which is the outcome of the multifractal distribution of singularities in real space.

The shape of the central part is a reflection of local structure of flow fields representing a wave and oscillation of vortex due to the interaction between vortices and so on.

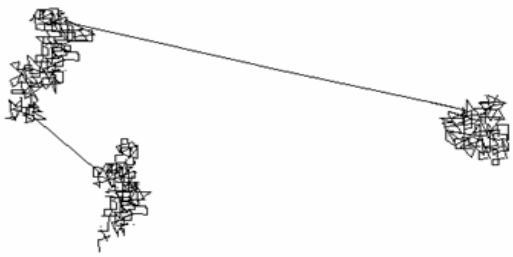

We expect that MPDFA can be a clue to search for the fundamental process of intermittency, i.e., the origin of singularities and the reason why the singularities distribute themselves multifractal way, etc., which may provide us with a fruitful insight to produce something for the dynamical approach.

It is one of the attractive future problems to find out two different dynamics, i.e., the one determines the tail part of PDF, and the other the central part of PDF.

When the underlying dynamics of MPDFA is revealed by starting the consideration with N-S equation, it may provide us with new route to extract intermittency from the dynamical point of view, e.g., an appropriate RG pathway to intermittency.

Toshihico Arimitsu (U of Tsukuba)
Naoko Arimitsu (Yokohama Nat'l U)
Kyo Yoshida (U of Tsukuba)
Hideaki Mouri (Inst. of Meteorology)

Thank you for your attention.